# Dynamics and switching processes for magnetic bubbles in nanoelements

C. Moutafis,[1] S. Komineas,[2] and J. A. C. Bland[1,*]
[1]*Cavendish Laboratory, J. J. Thomson Avenue, Cambridge CB3 0HE, United Kingdom*
[2]*Department of Applied Mathematics, University of Crete, Knossou Avenue, 71409 Heraklion Crete, Greece*
(Received 18 March 2009; revised manuscript received 22 May 2009; published 25 June 2009)

We study numerically the dynamics of a magnetic bubble in a disk-shaped magnetic element which is probed by a pulse of a magnetic field gradient. Magnetic bubbles are nontrivial magnetic configurations which are characterized by a topological (skyrmion) number $\mathcal{N}$ and they have been observed in mesoscopic magnetic elements with strong perpendicular anisotropy. For weak fields we find a skew deflection of the axially symmetric $\mathcal{N}=1$ bubble and a subsequent periodic motion around the center of the dot. This gyrotropic motion of the magnetic bubble is shown here for the first time. Stronger fields induce switching of the $\mathcal{N}=1$ bubble to a bubble which contains a pair of Bloch lines and has $\mathcal{N}=0$. The $\mathcal{N}=0$ bubble can be switched back to a $\mathcal{N}=1$ bubble by applying again an external field gradient. Detailed features of the unusual bubble dynamics are described by employing the skyrmion number and the moments of the associated topological density.

DOI: 10.1103/PhysRevB.79.224429 PACS number(s): 75.70.Kw, 75.60.Ch, 75.75.+a, 12.39.Dc

## I. INTRODUCTION

Magnetic bubbles are observed as spots of opposite magnetization in an otherwise uniformly magnetized film. They were studied extensively since their first observation in the 1960s in ferromagnetic films with perpendicular anisotropy.[1,2] The statics and dynamics of magnetic bubbles proved to be a subject of surprising complexity. One of the most interesting phenomena is their response to an external inhomogeneous field. In a counterintuitive way, they are known to be deflected at an angle to an external magnetic field gradient. This was shown to be directly connected to their nontrivial topological structure. They carry a topological number called the skyrmion number which enters in a collective coordinate description of bubble dynamics.[3,4]

In the last years, it was shown experimentally that single magnetic bubbles can be sustained in disk-shaped magnetic elements with perpendicular anisotropy.[5–7] Although these have the same gross features and the same topological structure as their counterparts in films, their statics is significantly different. Magnetic bubbles in disk elements are sustained without an external field and they may be ground magnetic states for magnetic elements of appropriate sizes.[8–10] A detailed study of magnetic bubbles in FePt nanodots was carried out in Ref. 7 using numerics and magnetic-force microscopy (MFM) imaging of arrays of dots with various diameters. In particular, almost circular magnetic bubbles confined in the center of the dots were observed as a common bidomain state in sufficiently small dots. Tridomain states which have the form of concentric rings with alternating magnetization were also observed, and they can be interpreted as multidomain magnetic bubbles.

The extensive experimental research of the last years on topologically nontrivial structures in magnetic nanoelements has focused largely on magnetic vortices. These are spontaneously created in magnetic elements with no or a small magnetic anisotropy. The dynamics of vortices has been observed in time-resolved experiments which revealed the profound role of the vortex polarity on their dynamics.[11] This means that the vortex topological structure is closely related to their dynamics, as also noted above for magnetic bubbles.

In the present paper we shall focus on bubble dynamics in magnetic nanoelements. The observations of magnetic bubbles of various topological structures[7] suggest that perpendicular anisotropy dots can be used to significantly widen the scope for dynamical experiments in ferromagnetic elements, beyond the current work on vortex dynamics. We expect an unusual dynamical behavior. The dynamics of bubbles should be expected to bear similarities to that of vortices because they both carry a nonzero skyrmion number. It is one of the aims of the present work to emphasize that similarities in dynamics can be traced to similarities in topological structures. Our study of the details of bubble dynamics in magnetic nanoelements is motivated by interest in fundamental processes in the magnet as well as by the potential of magnetic elements for technological applications.

The paper is organized as follows. In Sec. II we discuss the bubble skyrmion number and its relation to dynamics. In Sec. III we present our results on the dynamics of a bubble with skyrmion number unity and show that it exhibits gyrotropic motion. In Sec. IV we show that a bubble with skyrmion number unity can be switched to a different bubble with skyrmion number zero. In Sec. V we show that a bubble with skyrmion number zero can be switched back to one with skyrmion number unity. The last Sec. VI contains our concluding remarks.

## II. BUBBLE DYNAMICS AND TOPOLOGY

The dynamics of the magnetization vector $\boldsymbol{M}$ is given by the Landau-Lifshitz (LL) equation with a Gilbert damping term. We suppose a material with saturation magnetization $M_s$, exchange constant $A$, and a uniaxial perpendicular anisotropy with constant $K$. In a rationalized form the LL equation can be written as

$$\frac{\partial \boldsymbol{m}}{\partial \tau} = -\alpha_1 \boldsymbol{m} \times \boldsymbol{f} - \alpha_2 \boldsymbol{m} \times (\boldsymbol{m} \times \boldsymbol{f}),$$

 

$$\boldsymbol{f} \equiv \Delta \boldsymbol{m} - Q m_z \hat{\boldsymbol{e}}_z + \boldsymbol{h} + \boldsymbol{h}_{\text{ext}}, \tag{1}$$

where $\boldsymbol{m} \equiv \boldsymbol{M}/M_s$ is the normalized magnetization, $\boldsymbol{h} \equiv \boldsymbol{H}/M_s$ and $\boldsymbol{h}_{\text{ext}} \equiv \boldsymbol{H}_{\text{ext}}/M_s$ are the normalized magnetostatic and external fields, $Q \equiv 2K/(\mu_0 M_s^2)$ is the quality factor, and $\hat{\boldsymbol{e}}_z$ is the unit vector in the third ($z$) magnetization direction (taken to be the easy axis). If $\alpha$ is the dissipation constant then $\alpha_1 \equiv 1/(1+\alpha^2)$, $\alpha_2 \equiv \alpha/(1+\alpha^2)$. The length and time units in Eq. (1) are

$$\ell_{\text{ex}} \equiv \sqrt{2A/(\mu_0 M_s^2)}, \quad \tau_0 \equiv 1/(\gamma M_s), \tag{2}$$

where $\gamma$ is the gyromagnetic ratio and we will present our results in these units.

In the next sections we perform numerical simulations based on the LL equation using the OOMMF micromagnetics simulator.[12] We typically use the parameter values $M_s = 10^6$ A/m, $A = 10^{-11}$ J/m, and $K = 1.3 \times 10^6$ J/m, which give

$$\ell_{\text{ex}} = 4 \text{ nm}, \quad \tau_0 = 4.5 \text{ ps}, \quad Q = 2.1. \tag{3}$$

These correspond to FePt, although the anisotropy value lies in the lower limit for this material. Our results (when quoted in units of $\ell_{\text{ex}}, \tau_0$) are independent of the specific numerical values.

A magnetic bubble is a circular domain of opposite magnetization in an otherwise uniformly magnetized film perpendicular to the film surface. In a magnetic element of submicrometer dimensions such a circular domain can be spontaneously created in the center of the particle and it is a remanent state.[5–7] The magnetic bubble has a nontrivial topological structure which is only revealed when we consider the in-plane magnetization components, or, in other words, the domain wall between the bubble domain [which we shall consider to point "down," i.e., $\boldsymbol{m} = (0,0,-1)$] and the periphery of the particle [which we shall consider to point "up," i.e., $\boldsymbol{m} = (0,0,1)$].

The complexity of the magnetization configuration can be quantified by a topological invariant called the *skyrmion number*. This is defined as

$$\mathcal{N} = \frac{1}{4\pi} \int n dx dy, \quad n \equiv \frac{1}{2} \epsilon_{\mu\nu} (\partial_\nu \boldsymbol{m} \times \partial_\mu \boldsymbol{m}) \cdot \boldsymbol{m}, \tag{4}$$

where $\epsilon_{\mu\nu}$ is the antisymmetric tensor ($\mu, \nu = 1,2$) and $n$ is a *topological density* which is integrated over the plane. The integration gives an integer value for $\mathcal{N}$ in the case of an infinite two-dimensional medium where the magnetization $\boldsymbol{m}$ goes to a constant value at spatial infinity. We expect a deviation from this rule for the present case of a magnetic element. For the purposes of the present paper we shall consider that the plane of integration is the top surface of a disk element. The result for $\mathcal{N}$ depends in general on the choice of the plane of integration. However, we expect that the magnetization vector takes the value $\boldsymbol{m} \approx (0,0,1)$ on the side surface of the particle. This would guarantee that the integral given in Eq. (4) will be almost independent of the plane of integration and the value of $\mathcal{N}$ will be close to an integer. Indeed, $\mathcal{N}$ is very close to an integer for materials with very strong anisotropy, as is the case in the present work, (see Ref. 7 for numerical solutions for such bubbles). In the case of weaker anisotropy[5,6] significant deviations from an integer value may occur depending on the specific parameters of the system (see Ref. 10 for numerical solutions for the latter bubbles). A noninteger value of $\mathcal{N}$ may not change significantly the picture for bubble dynamics but it would make the theoretical analysis more complicated.

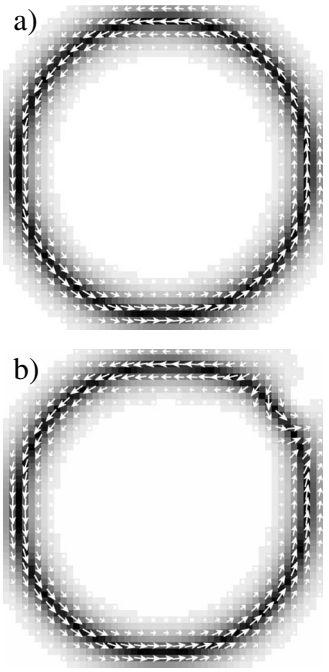


FIG. 1. Bubbles with (a) $\mathcal{N}=1$ and (b) $\mathcal{N}=0$. Only the domain wall is shown. We suppose that the magnetization points down inside the wall while it points up outside it.

The magnetic bubbles observed in Refs. 5–7 are most likely axially symmetric, according to symmetry and energy arguments, and they therefore have $\mathcal{N}=1$.[9] Such a bubble is shown in Fig. 1(a). A different bubble with $\mathcal{N}=0$ is shown in Fig. 1(b) and the differences in the domain walls of the two bubbles are obvious. It is useful to note here that the skyrmion number of a vortex takes half-integer values. This is $\mathcal{N} = \pm 1/2$ for almost all vortices commonly observed in magnetically soft dots, where the sign depends on the vortex "polarity" (that is, the direction of the magnetization in the vortex center).

The skyrmion number $\mathcal{N}$ is directly related to the magnetization dynamics as has been seen in many experiments.[1,2] This effect has been studied in Ref. 3 where a collective coordinate model for bubble dynamics is expressed with the use of the "gyrocoupling vector," whose length is a quantity proportional to $\mathcal{N}$. The dynamical properties of topological solitons in two-dimensional ferromagnets with uniaxial anisotropy were later considered in Ref. 13. Furthermore, the skyrmion number has direct implications for the unambiguous definition of conservation laws (e.g., the linear momentum) for the Landau-Lifshitz equation.[14,15] The profound effect of the skyrmion number on vortex dynamics can be seen in recent experiments. For example, the effect of vortex polarity has been studied in Refs. 11 and 16.

In the literature extensive use has been made of a topological number called the winding number $S$. This gives the

number of times that the magnetization vector winds around a full circle as we trace a circle around the center of a vortex or a bubble. For simple structures (such as vortices or the bubbles studied in this paper) $S$ is related to $\mathcal{N}$ through the simple relation, i.e., $\mathcal{N}=-1/2Sp$, that is, $\mathcal{N}$ depends both on $S$ as well as on the vortex or bubble polarity $p$. For more complicated topological solitons there is no simple relation between the two topological numbers.

### III. GYROTROPIC DYNAMICS OF THE $\mathcal{N}=1$ BUBBLE

We perform numerical simulations based on the LL equation using the OOMMF micromagnetics simulator.[12] We simulate a magnetic bubble in a disk-shaped magnetic element with diameter $D=40\ell_{\mathrm{ex}}$ (160 nm) and thickness $t=8\ell_{\mathrm{ex}}$ (32 nm). We discretize space on the $(x,y)$ plane using a lattice spacing $\delta x=\delta y=0.4\ell_{\mathrm{ex}}$ (1.6 nm) and assume uniform magnetization along the axis of the disk, which is taken to be in the third $(z)$ direction. We start the micromagnetics simulator using as an initial configuration a crude model for a $\mathcal{N}=1$ bubble. In terms of the components of the magnetization in cylindrical coordinates this is

$$(m_\rho,m_\phi,m_z)=\begin{cases}(0,0,-1), & \rho\leq R_a,\\ (0,1,0), & R_a<\rho<R_b,\\ (0,0,1), & \rho\geq R_b,\end{cases} \tag{5}$$

where $\rho$ is the radial coordinate, $R_a$ and $R_b$ are constants and they have typically been chosen as $R_a=0.4D$ and $R_b=0.55D$. It points down in the dot center, up in the dot periphery, and azimuthally in the domain wall between the two domains, which is located at $R_a<\rho<R_b$. In our first numerical simulation, we evolve Eq. (1) in time using a large dissipation constant and we eventually obtain a static magnetic bubble as a remanent state. This is a circular domain at the center of the dot, which is surrounded by a domain wall.[7,9] The magnetic configuration is axially symmetric, i.e., the magnetization components $m_\rho,m_\phi,m_z$ depend on the cylindrical coordinates $\rho$ and $z$ only. Such a configuration has a skyrmion number $\mathcal{N}=1$ and it is shown in Fig. 1(a).

We aim to study the dynamical behavior of the magnetic bubble described in the preceding paragraph. For this purpose we apply an external magnetic field pointing along the perpendicular direction $z$. The simplest choice would be a uniform external field but this would merely make the bubble shrink or expand.[9] Here, we rather aim to study the bubble motion when this is shifted from its equilibrium position at the dot center. This can be achieved by an external magnetic-field gradient, as has been shown in the work for magnetic bubbles in continuous films.[1,2] We choose a field with a gradient along the $x$ direction, i.e.,

$$\boldsymbol{h}_{\mathrm{ext}}=(0,0,h_{\mathrm{ext}}),\quad h_{\mathrm{ext}}=gx, \tag{6}$$

where $g$ is the dimensionless strength of the gradient. Such a field generates a corresponding gradient of the external field energy. One would expect a translation of the bubble along the field gradient, i.e., along the $x$ direction. The detailed numerical simulation does, however, show quite different dynamics than this expectation as will be explained in the following.

We evidently need to follow the bubble position in order to measure the effect of the external field gradient. There is no obvious absolute measure of this position but various measures can be defined. A relatively simple one is given by the following moments of the magnetization:

$$X=\frac{\int x(m_z-1)dV}{\int (m_z-1)dV},\quad Y=\frac{\int y(m_z-1)dV}{\int (m_z-1)dV}, \tag{7}$$

which give the mean position of the bubble domain (where $m_z=-1$ and $M_z=-M_s$). Another measure of the bubble position is defined as[14]

$$R_x=\frac{\int xndV}{\int ndV},\quad R_y=\frac{\int yndV}{\int ndV}, \tag{8}$$

where $n$ is the topological density defined in Eq. (4). Equation (8) gives the location of the nontrivial topological structure of the bubble. This is referred to as the *guiding center* of the bubble. The latter definition is obviously only valid when $\mathcal{N}\neq 0$. The moments of the topological density [Eq. (8)] are significant for the dynamics as they are proportional to the components of the linear momentum of the magnetization field within the LL equation. Their short-time behavior gives a qualitatively correct description of the unusual skew deflection of magnetic bubbles under a field gradient.[14,15]

In the series of numerical simulations which we present in the following we use as an initial condition the static magnetic bubble in the dot center which we have previously found. We apply the external magnetic field [Eq. (6)], choose a realistic dissipation constant $\alpha=0.01$, and follow the dynamics of the bubble in time, as given by the LL Eq. (1). The strength of the field gradient, in this simulation, is chosen to be $g=-0.0025$. This value practically means that the external field is $h_{\mathrm{ext}}=0.05M_s$ at the left end of the dot (at $x=-D/2=-20\ell_{\mathrm{ex}}$) and it is gradually reduced to become $h_{\mathrm{ext}}=-0.05M_s$ at the right end of the dot (at $x=D/2=20\ell_{\mathrm{ex}}$). The field is applied for a time period of $\tau=44.5\tau_0$ (200 ps) and it is then switched off completely.

The bubble orbit as given by the moments of the magnetization [Eq. (7)] and also by the moments of the topological density [Eq. (8)] is shown in Fig. 2. During the application of the external field, the moments [Eq. (7)] give a skew deflection of the bubble with respect to the field gradient toward the first quadrant. The moments [Eq. (8)] indicate more clearly a motion along the direction perpendicular to the field gradient during the initial stages of the simulation. It is impressive that $R_y$ appears to follow a rectilinear motion for times $\tau<11\tau_0$ (50 ps) with a measured velocity

$$\left(\frac{dR_x}{d\tau},\frac{dR_y}{d\tau}\right)\approx(0.0,0.095)\frac{\ell_{\mathrm{ex}}}{\tau_0}. \tag{9}$$

This dynamical behavior is anticipated by the results of Refs. 14 and 15, although it should be noted that those refer to infinite continuous films. The approach of the same refer-

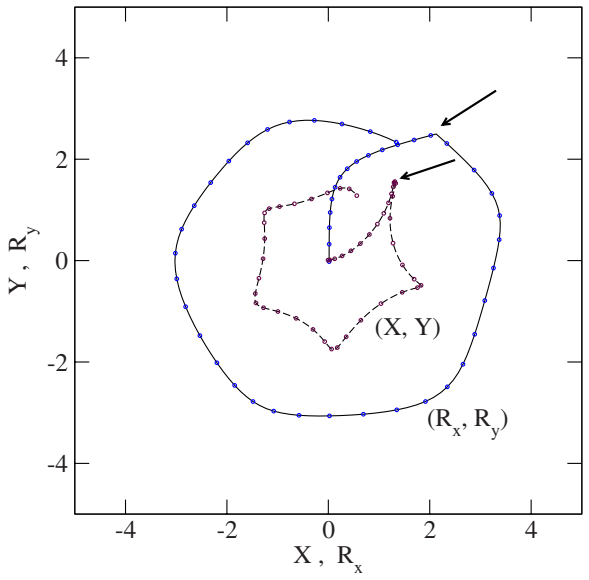


FIG. 2. (Color online) The orbit of the bubble under an external field gradient [Eq. (6)] with $g=-0.0025$. The solid line shows the coordinates $(R_x,R_y)$ of Eq. (8). The dashed line shows the coordinates $(X,Y)$ of Eq. (7). The circles mark the bubble position at times which are multiples of $5.33\tau_0$ (15 ps). The arrows indicate the point where the field is switched off.

ences has produced formulae for the initial velocity (at $\tau=0$) of the bubble. We reproduce these formulae in the present notation for convenience,

$$\frac{dR_x}{d\tau} = -\alpha_2 \frac{g\nu}{4\pi\mathcal{N}t}, \quad \frac{dR_y}{d\tau} = \alpha_1 \frac{g\mu}{4\pi\mathcal{N}t}, \tag{10}$$

where $t$ is the film thickness, $\mu$ is the total magnetization in the third direction, and $\nu$ is essentially the anisotropy energy,

$$\mu = \int (m_z - 1)dV, \quad \nu = \frac{1}{2}\int (1 - m_z^2)dV. \tag{11}$$

All quantities are measured in units [Eq. (2)]. In order to find numerical values, we substitute in Eq. (11) the configuration of the static bubble and find $\mu/t=-815$, $\nu/t=41$. We then obtain

$$\left(\frac{dR_x}{d\tau}, \frac{dR_y}{d\tau}\right) = (0.00008, 0.16)\frac{\ell_{ex}}{\tau_0}, \tag{12}$$

which clearly gives a deflection of the bubble perpendicular to the direction of the field gradient. The velocity $dR_y/d\tau$ is much larger than $dR_x/d\tau$ because $\alpha_1 \gg \alpha_2$ (for $\alpha=0.01$) and because the bubble total magnetization $\mu$ (which is proportional to the bubble area) is much larger than its anisotropy energy $\nu$ (which is proportional to the length of the bubble domain wall).

The result in Eq. (12) gives correctly the tendency of $(R_x,R_y)$ to move along the $y$ direction, although the calculated velocity value is about 60% in error. However, one should keep in mind that Eq. (10) was derived for infinite films and they hold only at the very beginning of the process.

When the external field is switched off at $\tau=44.5\tau_0$ (200 ps) the bubble is in the first quadrant at $(R_x,R_y)=(2.1,2.5)\ell_{ex}$ while $(X,Y)=(1.3,1.6)\ell_{ex}$. We then observe an almost circular motion of the $(R_x,R_y)$ orbit of the particle with a radius $\sim 3\ell_{ex}$. The type of motion for $(X,Y)$ is more involved and its trajectory is roughly a pentagon, as seen in Fig. 2. The period of this almost periodic motion is approximately $T=230\tau_0$ (1 ns) (i.e., frequency $f=1$ GHz).

The bubble, certainly, does not move as a rigid body around the dot center. The details of its motion can be seen in the three snapshots presented in Fig. 3. The initial state is shown in Fig. 3(a). [This is the same configuration as in Fig. 1(a) except that the whole element is shown now.] Figure 3(b) shows the configuration at time $\tau=44.5\tau_0$, that is, at the end of the application of the external field. While the bubble preserves its general structure it has apparently shifted to the first quadrant. Figure 3(c) shows the bubble at time $\tau=267\tau_0$ (1200 ps) when it has almost completed a full circle. The deformation of the bubble is small and also the details of the domain-wall structure are preserved. However, such a coherent motion does not happen for large field gradients as will be explained in the next section.

We have also repeated the simulation with a stronger field gradient $g=-0.005$. The results are similar to those described in the preceding paragraphs. The initial velocity for the bubble is now $dR_y/d\tau=0.19$, i.e., twice the value given in Eq. (9). Thus the bubble velocity seems to be proportional to $g$ in agreement with the prediction of Eq. (10). The bubble is

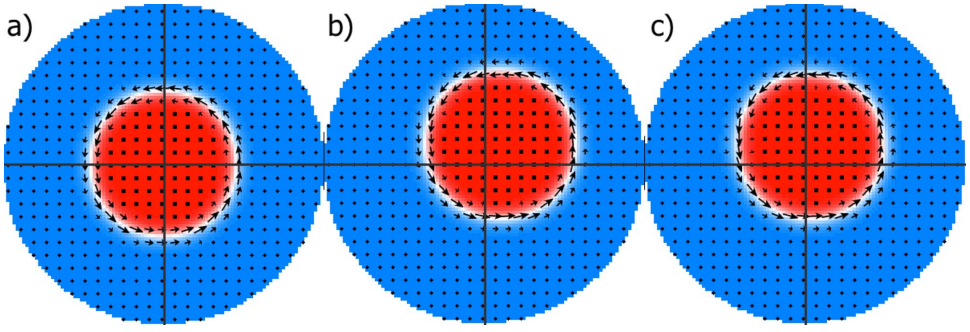


FIG. 3. (Color online) Snapshots from the simulation for a bubble with $\mathcal{N}=1$ under external field gradient [Eq. (6)] with $g=-0.0025$. They show the bubble (a) at the dot center (at time $\tau=0$), (b) when the external field is switched off [$\tau=44.5\tau_0$(200 ps)], and (c) when this has completed a cycle around the dot center [$\tau=267\tau_0$(1200 ps)].

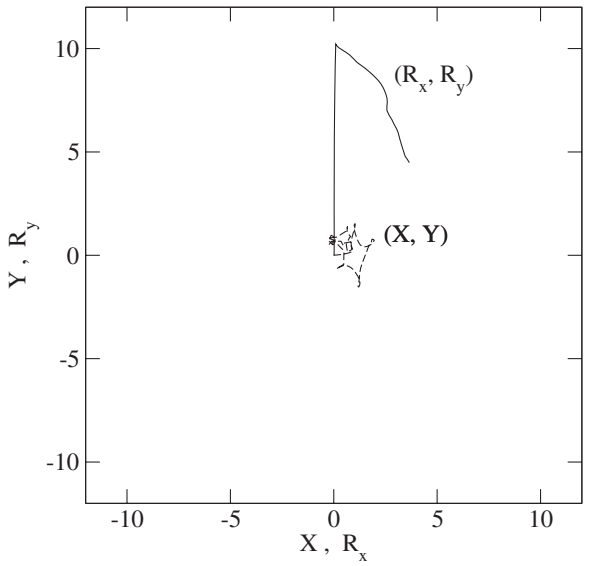


FIG. 4. The trajectory of the bubble under external field gradient [Eq. (6)] with $g=-0.025$. The solid line shows the coordinates $(R_x,R_y)$ of Eq. (8). They have been traced until $\tau=85.5\tau_0$ when we have switching. The dashed line shows the coordinates $(X,Y)$ of Eq. (7), which have been traced until $\tau=432\tau_0$.

later set in a circular motion around the center of the dot. The period of this motion is similar to that given in the $g=-0.0025$ case (i.e., $T\approx 1$ ns), although we obtain a displacement of the bubble from the dot center significantly larger, roughly twice that shown in Fig. 2.

## IV. SWITCHING OF THE $\mathcal{N}=1$ BUBBLE

We further study the response of the magnetic bubble to field gradients larger than those used in the previous section. We typically use in this section a large field-gradient strength $g=-0.025$. The field is applied only until $\tau=10\tau_0$ (45 ps). At initial times the coordinate $R_y$ is rapidly increasing while $R_x$ remains almost zero for $\tau<10\tau_0$. This motion is shown in Fig. 4. We observe a linear increase in $R_y$ until the field is switched off. The measured velocity $dR_y/d\tau=1.0$ is approximately ten times larger than the velocity found for $g=-0.0025$ in the previous section. This shows that $dR_y/d\tau$ is proportional to $g$. The velocity predicted by Eq. (10) is $dR_y/d\tau=1.6$ and it is roughly in agreement with the numerical results (as discussed in the $g=-0.0025$ case).

The position vector $(X,Y)$ is displaced from the origin by a small distance $\sim 1\ell_{\mathrm{ex}}$, as seen in Fig. 4. This is a much shorter distance than that observed in the previous section (see Fig. 2). This is because the field gradient is now applied for a much shorter time. Unlike the velocity for $(R_x,R_y)$, the velocity for the coordinates $(X,Y)$ is apparently not proportional to the strength of the field gradient $g$.

After the external field gradient is switched off the position of the bubble, measured by $(R_x,R_y)$, takes a sharp turn and appears to start a cyclic motion around the dot center similar to what was described in Sec. III. On the other hand, the coordinates $(X,Y)$ follow a nonregular path close to the dot center. Figure 5 shows snapshots of the simulation. At

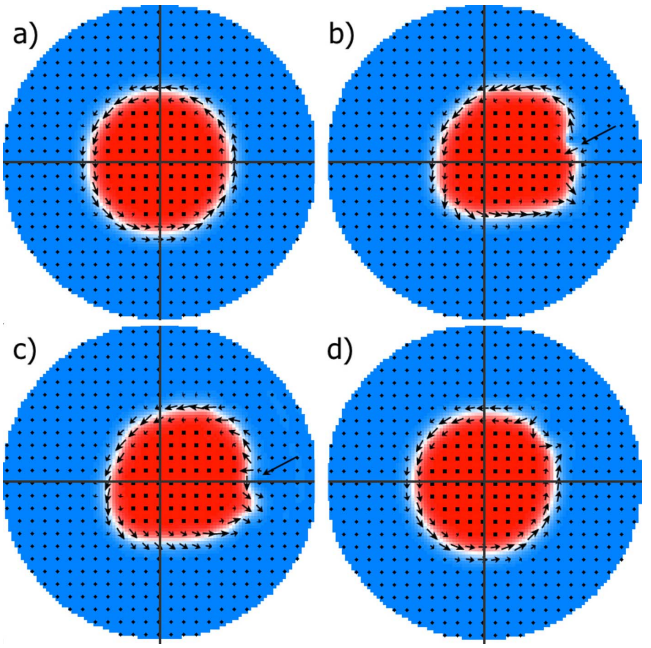


FIG. 5. (Color online) Snapshots from the simulation for a bubble under external field gradient [Eq. (6)] with $g=-0.025$. (a) A remanent $\mathcal{N}=1$ bubble in the dot center ($\tau=0$), (b) the instant just before the wall unwinding [$\tau=83\tau_0$(375 ps)], where the arrow indicates the area where the VBLs have developed, (c) the instant just after the wall unwinding [$\tau=85.5\tau_0$(385 ps)], where the arrow indicates the same area as in the previous entry, and (d) a $\mathcal{N}=0$ bubble as a remanent state (at the end of the simulation).

some later time significant gradients of the magnetization vector develop at the bubble domain wall. For example, at $\tau=83\tau_0$ (375 ps) [Fig. 5(b)] a part of the wall includes so-called vertical Bloch lines (VBLs).[1] At $\tau=85.5\tau_0$ (385 ps) an abrupt change in the magnetization occurs at the region of the domain wall where the VBLs had developed. This is accompanied by a burst of spin waves. Figure 5(c) shows the bubble after the domain wall has changed. Figure 6 shows magnifications of a part of the bubble corresponding to Figs. 5(b) and 5(c). A pair of VBLs is now part of the domain wall.

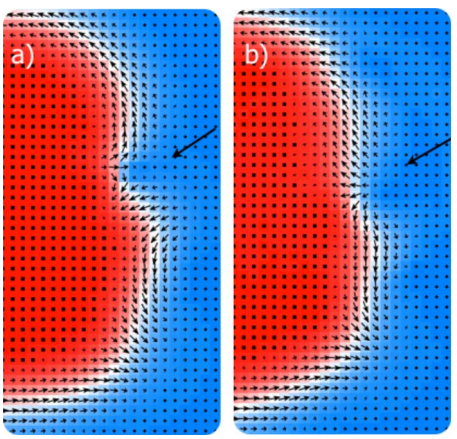


FIG. 6. (Color online) Blow ups of a part of the bubble which contains Bloch lines for (a) Fig. 5(b) and (b) Fig. 5(c) (the arrows correspond to those in Fig. 5).

Configurations with VBLs have been studied within the context of bubbles in films as reviewed in Ref. 1. A pair of VBLs can be winding when the magnetization winds by $2\pi$ radians as we move across them in the domain wall or nonwinding when the magnetization has a local net winding of zero (including a $\pi$ and $-\pi$ winding as we move across the wall).[1] The pair in Fig. 6(b) is a winding pair.

The transformation of the initial VBLs to a single pair of VBLs is a discontinuous process. Such discontinuous processes are normally impossible to induce because an infinite energy barrier would have to be overcome. In magnetic systems the energy barrier would be due to the exchange energy at regions with large magnetization gradients. However, the exchange energy of a two-dimensional magnetization configuration (e.g., a pair of VBLs) as this is shrinking is a finite constant. This is due to the scale invariance of the exchange energy in two dimensions (for example, see Refs. 17 and 18). Since the bubble is a quasi-two-dimensional magnetic configuration the exchange energy in the region of the approaching VBLs will not give an infinite energy barrier.

We should note here that a discontinuous change in the magnetization cannot, in principle, be described by micromagnetics on a discrete numerical mesh. However, since in the present case no singularities in the energy are involved, one could argue, at least heuristically, that the numerical solution on the discrete lattice does simulate correctly the process which actually occurs in the atomic lattice of the material. Such discountinuous changes have been reported in experiments in films.[1]

Although the magnetic bubble seems to remain intact in the dot even after the modification of the domain wall, a dramatic change has indeed occurred at the microscopic level. To show this we calculate the skyrmion number Eq. (4) of the magnetization. This is very close to unity for the initial bubble and it remains almost constant until the discontinuous change in the magnetic configuration occurs. At time $\tau=85.5\tau_0$ the skyrmion number $\mathcal{N}$ changes almost instantly to a value close to zero. Thus the discontinuous nature of the process of the annihilation of VBLs is reflected in an abrupt change from $\mathcal{N}=1$ to $\mathcal{N}=0$. The magnetic bubble with $\mathcal{N}=0$ is essentially different than the initial bubble with $\mathcal{N}=1$.

The coordinates $(R_x,R_y)$ do not give a well-defined measure of the bubble position for $\mathcal{N}=0$ since the denominators in Eq. (8) vanish. The bubble position can be followed by the coordinates $(X,Y)$ which are shown in Fig. 4. These take small values and they follow an orbit which is complicated and not a periodic one. That is, there is no trace of a gyrotropic (circular) motion of the bubble around the dot center, in contrast to the case of the $\mathcal{N}=1$ bubble. We relegate further discussion of this point until the end of the next section.

For longer times the system will relax to a remanent state due to dissipation. Since the relaxation process with our standard dissipation constant $\alpha=0.01$ takes prohibitively long simulation time, we actually use (for times well after $\tau=85.5\tau_0$) a large $\alpha=1$ only for the purpose of quickly finding the remanent state. The process of Fig. 5 eventually relaxes to an almost cylindrical bubble with $\mathcal{N}=0$ in the dot center shown in Fig. 5(d). The domain wall of the latter bubble is shown more clearly in Fig. 1(b), where a pair of winding VBLs is seen. The two VBLs apparently attract each other due to their magnetostatic field. We further discuss the details of the $\mathcal{N}=0$ bubble in the next section.

In conclusion, the application of a strong magnetic-field gradient on a dot which is in a bubble state with $\mathcal{N}=1$ has eventually switched it to a bubble with $\mathcal{N}=0$. We add that the field-gradient value $g=-0.025$ used in this section is indicative. We have also tried a field gradient $g=-0.0125$ and have obtained the switching process. Furthermore, we have achieved switching events while keeping the same field gradient ($g=-0.025$) but for different field-pulse durations.

Switching of the $\mathcal{N}=1$ magnetic bubble into a $\mathcal{N}=0$ bubble has apparently been observed for the first time in Ref. 19. A garnet film was used which was exchange coupled to a magnetic layer. Apart from the bias field (which is necessary in order to sustain a bubble in a film) an in-plane field was applied. On top of these fields, 100 ns long pulses of a field gradient perpendicular to the film were applied which led to bubble switching. In other experiments with bubbles in continuous films changes in bubble dynamics have been observed which have been attributed to changes in the bubble skyrmion number.[2]

## V. SWITCHING OF THE $\mathcal{N}=0$ BUBBLE

The $\mathcal{N}=0$ bubble was shown to be a remanent magnetic state and we are therefore motivated to study it on its own right. The $\mathcal{N}=1$ bubble has energy $E=2.797\times10^{-16}$ J while the $\mathcal{N}=0$ bubble has $E=2.824\times10^{-16}$ J. Thus the latter is an excited metastable state. Its domain wall contains a pair of winding VBLs which are located close together. Magnetic charges are accumulated around the VBLs, thus creating a strong magnetostatic field in their vicinity.

We study in this section the dynamics of a $\mathcal{N}=0$ bubble in a nanodisc, following a procedure analogous to that in Sec. IV. We perform numerical simulations using the remanent bubble state, in the dot center, with skyrmion number $\mathcal{N}=0$ [i.e., the state shown in Figs. 5(d) and 1(b)]. We apply a strong field gradient [Eq. (6)] with $g=-0.025$. The field is switched off at time $\tau=55\tau_0$ (250 ps). We observe that the bubble is displaced from the center of the dot. The orbit of the bubble as given by the moments of Eq. (7) is shown by the dashed line in Fig. 7. It moves in the first quadrant under the influence of the field.

The structure of the bubble domain wall is getting increasingly complicated under the influence of the field gradient as the pair of winding VBLs are drifting around the wall. The complicated dynamics of the domain wall continues even after the field is switched off. Figure 8 shows snapshots of the simulation. At time $\tau=95.5\tau_0$ (430 ps) we observe that the two VBLs come close together [Fig. 8(b)] and thus large magnetization gradients develop in a very short region of the domain wall (indicated by an arrow). Figure 9(a) shows a magnification of the part of the domain wall which contains the pair of VBLs. This leads to annihilation of the pair of VBLs as shown in Fig. 8(c) at time $\tau=98\tau_0$ (440 ps). Figure 9(a) shows that the VBLs have become adjacent just before the annihilation while Fig. 9(b) shows a magnification of the part of the domain wall where the VBL pair annihilation took place.

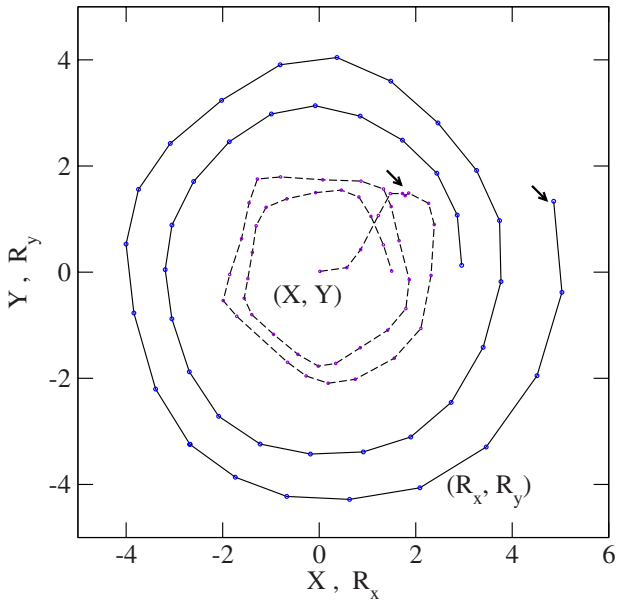


FIG. 7. (Color online) The trajectory of a $\mathcal{N}=0$ bubble which is subject to an external field [Eq. (6)] with $g=-0.025$. The field is switched off at $\tau=55\tau_0$ (250 ps). The bubble switches to a $\mathcal{N}=1$ bubble at $\tau=98\tau_0$ (440 ps), which is indicated by the arrows. We plot both the coordinates [Eq. (8)] (solid line), which are defined only after the switching for $\mathcal{N}=1$, and the coordinates [Eq. (7)] (dashed line). The total simulation time is $\tau=555.5\tau_0$ (2.5 ns).

The annihilation of a pair of winding VBLs is a discontinuous process. As also mentioned in the previous section, such a process should be possible in the present two-dimensional bubble configurations.

The discontinuous nature of the process of annihilation of the pair of winding VBLs is reflected in an abrupt change in the skyrmion number from $\mathcal{N}=0$ to $\mathcal{N}=1$ which happens precisely at the time of the annihilation of VBLs. The $\mathcal{N}=1$ bubble is located off-center at the moment of its creation. The trajectory of the bubble as given by Eqs. (7) and (8) is shown in Fig. 7. We observe that once the skyrmion number becomes unity the bubble starts a circular motion around the dot center. The bubble motion is damped due to dissipation, it follows a spiraling orbit and it eventually remains static at the dot center. It is remarkable that the bubble motion is reflected in a rather smooth circular trajectory for the moments of the local vorticity (solid line) compared to an angled (nearly pentagonal) curve for the moments of $m_z$ (dashed line). The frequency of rotation is approximately 1 GHz. The above findings concerning the circular motion of the $\mathcal{N}=1$ bubble are fully consistent with the results reported in Sec. III.

The results of the present and the previous sections indicate differences between the dynamics of the $\mathcal{N}=0$ and the $\mathcal{N}=1$ bubble. We have shown that the $\mathcal{N}=1$ bubble, when this is not in the dot center, goes on a gyrotropic motion as seen in Figs. 2 and 7. The behavior of a $\mathcal{N}=0$ bubble is however less clear. We have seen in Sec. IV that the $\mathcal{N}=0$ bubble created during a dynamical process does not undergo a circular motion around the dot center. We did not clearly observe a gyrotropic motion for the $\mathcal{N}=0$ bubble in this section either. Further numerical simulations support these findings.

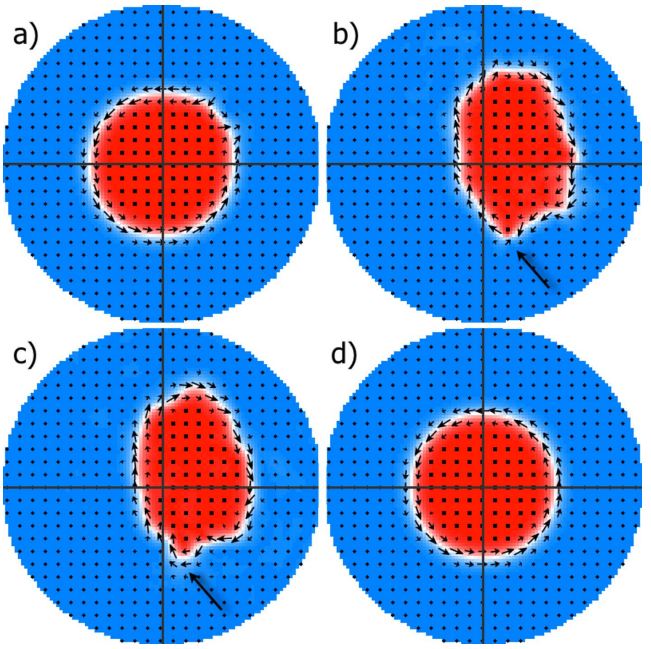


FIG. 8. (Color online) Snapshots from the simulation for a bubble under external field gradient [Eq. (6)] with $g=-0.025$. (a) A remanent $\mathcal{N}=0$ bubble in the dot center (at $\tau=0$), (b) the instant just before the wall unwinding where the arrow indicates the area where the VBLs have developed [$\tau=95.5\tau_0$(430 ps)], (c) the instant just after the wall unwinding where the arrow indicates the same area as in the previous entry [$\tau=98\tau_0$(440 ps)], and (d) the final results of the simulation, i.e., a static $\mathcal{N}=1$ bubble.

## VI. CONCLUSIONS

We have presented a numerical study for the unusual dynamical behavior of a bubble in a magnetic nanoelement under an external magnetic field gradient. It has been shown that a bubble with skyrmion number $\mathcal{N}=1$ is deflected at an angle to the field gradient. The details of this skew deflection of the bubble confirm previous theoretical studies. When the external field is switched off the bubble is set on a gyrotropic motion around the center of the nanoelement. Previous ex-

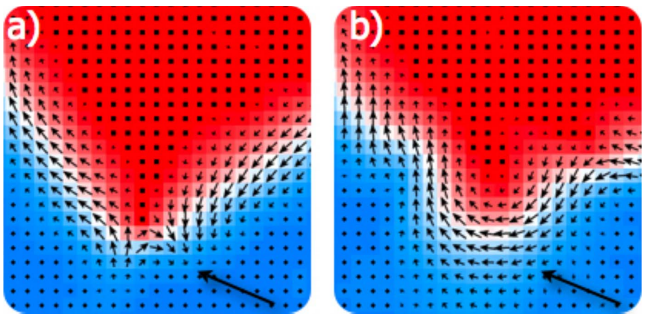


FIG. 9. (Color online) Blow ups of a part of the bubble corresponding to (a) Fig. 8(b) and (b) Fig. 8(c) (the arrows correspond to those in Fig. 8).

perimental and theoretical studies on this subject refer to the dynamical behavior of magnetic bubbles in infinite films. The present study has applied the idea of an external magnetic field gradient in the context of a magnetic bubble in a nanoelement.

A strong enough field gradient was shown to affect the bubble structure profoundly and it induced a switching of the $\mathcal{N}=1$ bubble to a bubble with skyrmion number $\mathcal{N}=0$. The latter is shown to be a remanent state of the magnetic system. Application of a similar field gradient to the $\mathcal{N}=0$ bubble induces a switching back to the original $\mathcal{N}=1$ bubble. The ultrafast switching between the two bubbles is achieved for times below one nanosecond which could prove to be a significant advantage for applications. Although the two bubbles look very similar regarding their perpendicular component of the magnetization they are essentially different magnetic states. We did not observe a simple gyrotropic motion of the $\mathcal{N}=0$ around the center of the nanoelement. However, the detailed features and especially the dynamics of this bubble need further investigation.

A dramatic difference between the dynamics of bubbles with $\mathcal{N}=0$ and $\mathcal{N}\neq 0$ is anticipated by earlier theoretical work. Thiele's equations for bubble dynamics[3] explicitly contain the skyrmion number $\mathcal{N}$. Furthermore, the skyrmion number has direct implications for the unambiguous definition of conservation laws (e.g., the linear momentum) for the Landau-Lifshitz equation.[14,15] Equation (10) has been derived based on the latter theory. Their denominators vanish for $\mathcal{N}=0$ thus implying that this should be treated as a separate special case.

In view of the extensive recent literature on the dynamics of a vortex in magnetic elements, our work extends the subject to other topological magnetic states such as magnetic bubbles. While almost all vortices observed so far have the same magnetization configuration, bubbles may have a variety of topological structures. This enriches the subject significantly and opens new possibilities not only for theoretical and experimental work but possibly also for technological applications. A systematic study for the excitation spectrum of bidomain and multidomain bubbles shows several interesting resonances indicating a variety of dynamical behaviors.[20,21]

## ACKNOWLEDGMENTS

C.M. thanks Emmanuel College and the Japanese Society for the Promotion of Science for financial support. S.K. acknowledges discussions with N. Papanicolaou.

*Deceased.

[1] A. P. Malozemoff and J. C. Slonczewski, *Magnetic Domain Walls in Bubble Materials* (Academic, New York, 1979).

[2] T. H. O'Dell, *Ferromagnetodynamics: The Dynamics of Magnetic Bubbles, Domains, and Domain Walls* (Wiley, New York, 1981).

[3] A. A. Thiele, Phys. Rev. Lett. **30**, 230 (1973).

[4] A. A. Thiele, J. Appl. Phys. **45**, 377 (1974).

[5] M. Hehn, K. Ounadjela, J. P. Bucher, F. Rousseaux, D. Decanini, B. Bartenlian, and C. Chappert, Science **272**, 1782 (1996).

[6] G. D. Skidmore, A. Kunz, C. E. Campbell, and E. D. Dahlberg, Phys. Rev. B **70**, 012410 (2004).

[7] C. Moutafis, S. Komineas, C. A. F. Vaz, J. A. C. Bland, T. Shima, T. Seki, and K. Takanashi, Phys. Rev. B **76**, 104426 (2007).

[8] J. K. Ha, R. Hertel, and J. Kirschner, Europhys. Lett. **64**, 810 (2003).

[9] S. Komineas, C. A. F. Vaz, J. A. C. Bland, and N. Papanicolaou, Phys. Rev. B **71**, 060405(R) (2005).

[10] C. Moutafis, S. Komineas, C. A. F. Vaz, J. A. C. Bland, and P. Eames, Phys. Rev. B **74**, 214406 (2006).

[11] S. B. Choe, Y. Acremann, A. Scholl, A. Bauer, A. Doran, J. Stöhr, and H. A. Padmore, Science **304**, 420 (2004).

[12] OOMMF User's Guide, Version 1.0, M. J. Donahue and D. G. Porter, Interagency Report No. NISTIR 6376, National Institute of Standards and Technology, Gaithersburg, MD, 1999, http://math.nist.gov/oommf

[13] B. A. Ivanov and V. A. Stephanovich, Phys. Lett. A **141**, 89 (1989).

[14] N. Papanicolaou and T. N. Tomaras, Nucl. Phys. B **360**, 425 (1991).

[15] S. Komineas and N. Papanicolaou, Physica D **99**, 81 (1996).

[16] K. S. Buchanan, P. E. Roy, M. Grimsditch, F. Y. Fradin, K. Yu. Guslienko, S. D. Bader, and V. Novosad, Nat. Phys. **1**, 172 (2005).

[17] O. A. Tretiakov and O. Tchernyshyov, Phys. Rev. B **75**, 012408 (2007).

[18] R. Rajaraman, *Solitons and Instantons* (North-Holland, Amsterdam, 1982).

[19] T. lin Hsu, AIP Conf. Proc. **24**, 624 (1975).

[20] N. Vukadinovic and F. Boust, Phys. Rev. B **75**, 014420 (2007).

[21] N. Vukadinovic and F. Boust, Phys. Rev. B **78**, 184411 (2008).